Comparative Medicine
Copyright 2015
by the American Association for Laboratory Animal Science

Vol 65, No 4
August 2015
Pages 295–307

*Original Research*

# Electrocardiographic Characterization of Cardiac Hypertrophy in Mice that Overexpress the ErbB2 Receptor Tyrosine Kinase

**Polina Sysa-Shah,[1] Lars L Sørensen,[2,3] M Roselle Abraham,[2] and Kathleen L Gabrielson[1*]**

**Electrocardiography is an important method for evaluation and risk stratification of patients with cardiac hypertrophy. We hypothesized that the recently developed transgenic mouse model of cardiac hypertrophy (ErbB2$^{tg}$) will display distinct ECG features, enabling WT (wild type) mice to be distinguished from transgenic mice without using conventional PCR genotyping. We evaluated more than 2000 mice and developed specific criteria for genotype determination by using cageside ECG, during which unanesthetized mice were manually restrained for less than 1 min. Compared with those from WT counterparts, the ECG recordings of ErbB2$^{tg}$ mice were characterized by higher P- and R-wave amplitudes, broader QRS complexes, inverted T waves, and ST interval depression. Pearson's correlation matrix analysis of combined WT and ErbB2$^{tg}$ data revealed significant correlation between heart weight and the ECG parameters of QT interval (corrected for heart rate), QRS interval, ST height, R amplitude, P amplitude, and PR interval. In addition, the left ventricular posterior wall thickness as determined by echocardiography correlated with ECG-determined ST height, R amplitude, QRS interval; echocardiographic left ventricular mass correlated with ECG-determined ST height and PR interval. In summary, we have determined phenotypic ECG criteria to differentiate ErbB2$^{tg}$ from WT genotypes in 98.8% of mice. This inexpensive and time-efficient ECG-based phenotypic method might be applied to differentiate between genotypes in other rodent models of cardiac hypertrophy. Furthermore, with appropriate modifications, this method might be translated for use in other species.**

**Abbreviations:** HCM, hypertrophic cardiomyopathy; LV, left ventricle; $QT_c$, QT interval corrected for heart rate.

Electrocardiography is an important method used in human patients for evaluation of cardiac hypertrophy, for example, hypertrophic cardiomyopathy (HCM).[30,35] Although echocardiography is considered to be the 'gold standard' in HCM diagnostics, ECG evaluation may provide additional information needed for diagnosis.[30] In some patients with HCM, ECG changes precede echocardiographic changes;[30,36] therefore the 2 modalities are often used together to screen family members of patients with HCM. Similarly, there are reports of athletes who suddenly die during training, in whom HCM was confirmed at autopsy and in whom ECG abnormalities were recorded in the absence of overt clinical signs.[23] In contrast, although developed before echocardiography, ECG is often underutilized in the characterization of mouse models of cardiac disease.

The first reports on mouse ECG were published in the 1950s[15,40] and were followed by the rapid development of rodent ECG methods, recording, and analysis.[16] Several approaches support the recording and analysis of mouse ECG, including 12-lead ECG,[7,51] open-chest models,[7,51] telemetry using radiofrequency transmitters,[16] and recording in anesthetized mice.[7,51] All of these methods provide information on cardiac electrophysiology, yet each has its specific advantages and limitations.[51] Further use of ECG in mouse models of cardiac disease could improve our understanding of the electrophysiologic remodeling in these diseases.

Several mouse models of HCM (due to genetic modifications of genes related to human HCM[18,21,50] or to lysosomal storage disease-related cardiomyopathies[2,4,6,46]) were developed to study these hypertrophic conditions and the resulting electrical disturbances in the myocardium. However, despite carrying the same genetic alterations that cause human disease, many mouse models do not have phenotypic ECG changes or even hypertrophy.[18,21,50] Therefore the development of a small animal model of cardiac hypertrophy with ECG features similar to those in human patients is of particular interest. We recently developed a mouse model with cardiac hypertrophy and pathologic features compatible with HCM[47] and hypothesized that various electrocardiographic features could enable us to distinguish between wildtype (WT) mice and transgenic littermates after weaning. In the current study, we established an ECG method that identifies the hypertrophic phenotype and thus assists in determining the genotype of mice. This ECG method thus reduced laboratory

*Received: 10 Oct 2014. Revision requested: 23 Nov 2014. Accepted: 06 Apr 2015.*
*[1]Department of Molecular and Comparative Pathobiology, Johns Hopkins Medical Institutions, Baltimore, Maryland, USA, [2]Department of Medicine, Division of Cardiology, Johns Hopkins University, Baltimore, Maryland, [3]Department of Cardiology, Gentofte Hospital, Copenhagen, Denmark*
** Corresponding author. Email: kgabriel@jhmi.edu*

costs and the time necessary to isolate and analyze DNA for genotyping.

## Materials and Methods

**Generation of ErbB2$^{tg}$ mice.** To investigate whether ErbB2 expression induced cardiac hypertrophy, we previously constructed 2 transgenic lines.[47] To this end, we first isolated rat *ErbB2* mRNA from brain and converted it to cDNA. The 5-kb cDNA fragment was subcloned into the *Bam*HI–*Sal*I site of the cardiac specific expression vector (α-myosin heavy-chain promoter) kindly provided by Dr Jeffrey Robbins (Molecular Cardiovascular Biology, Heart Institute, Cincinnati Children's Hospital Medical Center, Cincinnati, OH). Fertilized eggs from B6SJLF1/J mice were used for pronuclear microinjection of the DNA by the Johns Hopkins Transgenic Core Facility (Baltimore, MD). Founder animals were identified by PCR analysis and Southern blotting; 2 founder mice were used to develop 2 transgenic lines. Mice for these studies were housed in top-ventilated cages under a 12:12-h light:dark cycle with free access to food and water. Mice were negative for fur mites, pinworms, *Helicobacter* spp., mouse hepatitis virus, epidemic diarrhea of infant mice virus (rotavirus), minute virus of mice, mouse parvovirus types 1 and 2, mouse theilovirus, mouse adenovirus types 1 and 2, ectromelia virus, lymphocytic choriomeningitis virus, *Mycoplasma pulmonis*, pneumonia virus of mice, reovirus, Sendai virus, mouse norovirus, and mouse cytomegalovirus.

All studies were performed in strict accordance with the recommendations in the *Guide for the Care and Use of Laboratory Animals*.[17] The protocols for these studies were approved by the IACUC at the Johns Hopkins Medical Institutions.

**ECG studies** To characterize the in vivo electrophysiologic features, we performed ECG studies in unanesthetized WT and ErbB2$^{tg}$ littermates (age, 1 to 3 mo or 7 to 9 mo, depending on the study). The entire procedure was performed in approximately 1 min per mouse, without anesthesia. The ECG recordings were analyzed by a reviewer who was regarding the genotype of the mice (PSS).

Figure 1 A shows the manual restraint of a conscious mouse in the left hand. Using the right hand (not shown), the handler inserted 3 electrodes subcutaneously into right axilla right (black), right inguinal (green), and left inguinal (red) regions (lead II configuration; Figure 1 B) Lead II was used for most of the mice (approximately 95%) and was the first electrode configuration we selected to record data to determine phenotype. Lead I was used for the remaining mice, in which electrodes were placed in the right axilla (negative) and left axilla (positive) to better record the ECG of hearts with left-axis deviation (present in approximately 5% of transgenic mice). Lead III (electrode placement in the left axilla [negative] and left inguinal [positive] areas) was used rarely (less than 1% of recordings) to confirm the ECG phenotype in mice with unclear lead II and lead I recordings. Early in our development of the protocol, we anesthetized some mice (80 mg/kg ketamine and 10 mg/kg xylazine) when prolonged recording periods were needed.

The electrode needles used for this study were all 29-gauge recording needles (Figure 1 C) and were easily inserted under the skin. ECG recording was done at cageside in the hood next to cage racks. Restraining a mouse and inserting ECG electrodes is similar (in terms of the level of stress) as giving anesthesia subcutaneously or intraperitoneally.

In general, electrocardiograms were recorded for 5 to 10 s by using a PowerLab data acquisition system (model ML866, ADInstruments, Colorado Springs, CO) and Animal Bio Amp (model ML136, ADInstruments). The LabChart software (ADInstruments) allows for automated averaging of the recording by overlaying all the cycles recorded within defined time interval, by using QRS maximum (the tallest peak) or QRS minimum (the deepest peak) for the alignment. The resulting 'average' cycle was used for subsequent analysis. Thus, averaged standard ECG time intervals (RR, PR, QT) and waves (P, QRS complex, T) were detected and measured automatically. The ECG strain pattern was defined as a combination of downsloping convex ST segments with ST depression and inverted T waves opposite to the QRS axis.[41] The QRS interval was measured from the onset of the Q wave to the peak negative deflection of the S wave. The end of the QT interval was measured from the Q wave onset to the end of the negative portion of T wave; all QT intervals were corrected for heart rate according to a published formula (thus $QT_c$ hereafter).[29] ST segment is not clearly defined in mice, unlike in humans, whose ECG show a pause between the end of QRS and the start of the T wave.[14] Therefore, for consistency, we measured ST height according to the method provided by LabChart software, in which the measurement was taken at 10 ms after R wave peak and which served as an alignment point for beat-to-beat averaging. In one case, where software recognition of the ECG waves and intervals was incorrect, we manually measured parameters in a situation where the software incorrectly determined the P wave end at the beginning of the QRS complex instead of junction between the end of P wave deflection and isoelectric line; this situation was corrected by moving the marker for P wave end to the correct location.

**Echocardiography.** In vivo cardiac morphology and function were assessed echocardiographically by using a high-frequency, high-resolution ultrasound system (Vevo 2100, VisualSonics, Toronto, Canada) equipped with a 40-MHz transducer.[1] Briefly, mice were analyzed while at a plane of anesthesia (under 1% to 2% isoflurane) that did not depress the heart rate lower than 450 bpm and that provided optimal respiratory rates of 60 breaths per minute. Anesthesia was induced in mice by using an acrylic anesthesia box (VisualSonics); mice were moved to a custom imaging platform for maintenance of anesthesia by using a nose cone attached to a scavenging system. This platform contains a built-in ECG and surface thermometer system to continuously monitor heart rate and temperature during imaging. Body temperature was maintained at 37 °C, and a feedback system increased plate temperature when the temperature fell below 37 °C. Monitoring these parameters is important, because mice exposed to more than 2% isoflurane and body temperatures lower than 37 °C can develop bradycardia and depressed heart function.

The thicknesses of the left ventricular (LV) anterior and posterior walls were measured in short axis at papillary muscle level by using M-mode images, and LV mass was calculated from these measurements.[48] All echocardiography and image analysis was done by a single investigator (LLS), who was blinded in regard to genotype status.

To compare measurements obtained by ECG with those from echocardiography, echocardiographic studies were performed in 1- to 2-mo-old mice, followed 1 wk later by ECG recording and analysis. Data from WT and ErbB2$^{tg}$ mice were combined and used to evaluate the overall correlation of various ECG and

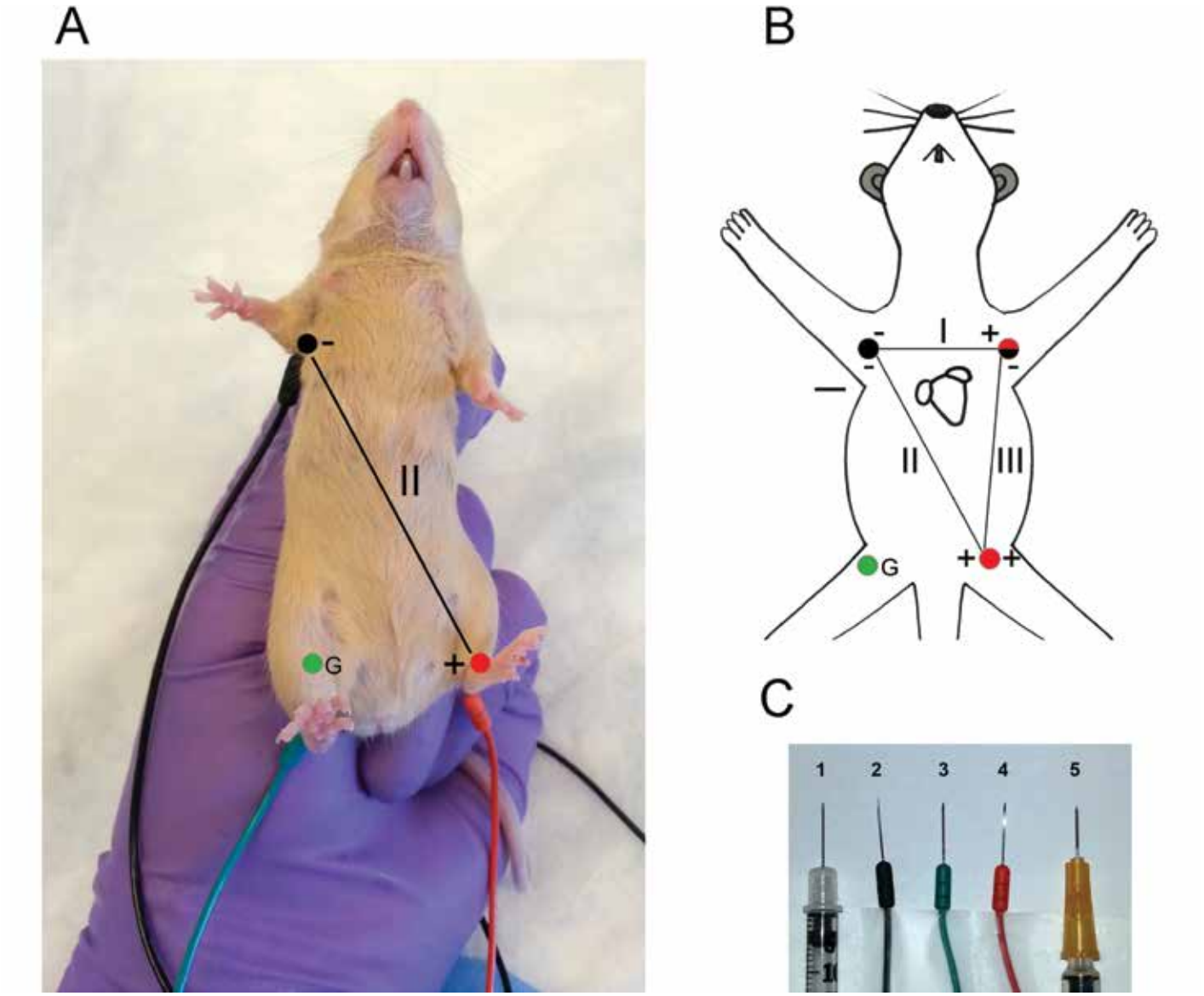


**Figure 1.** Electrocardiogram recording in an awake mouse. (A) Handling the mouse during ECG recording (electrodes are placed for the recording of the standard lead II). G, ground electrode (green). (B) The scheme of the electrodes placement for ECG recordings in a mouse: standard leads I, II, III. The placement of negative electrodes is indicated in black, and that of positive electrodes is marked in red. (C) ECG recording electrodes (2, 3, 4) with 28- (1) and 26- (2) gauge needles for comparison

echocardiographic parameters, whereas data for WT or ErbB2$^{tg}$ mice only were analyzed for the specific correlation between ECG and echocardiographic parameters in individual animals.

**Necropsy.** Mice were euthanized by $CO_2$; carcasses were weighed, and hearts were excised and weighed.

**Statistics.** Prism software (GraphPad, La Jolla, CA) was used to perform statistical analysis. Paired Student *t* tests were used to compare data from the same animal at different ages, and unpaired Student *t* tests were used to compare 2 unrelated groups of mice. To compare 3 or more groups, one-way ANOVA was performed. A *P* value of less than 0.05 was considered significant. Data are presented as mean ± 1 SD.

False-positive and false-negative results were determined by matching the ECG-predicted genotype with the genotype as confirmed by the heart weight measured at necropsy, the presence of distinctive myocardial disarray on review of pathology, or results of standard PCR-based genotyping assays. False-positive results were defined as mice that were transgenic according to ECG analysis but that whose heart weights were comparable to those of age-matched WT controls, with no myocardial disarray and negative PCR findings. False-negative results were defined as mice that were WT by ECG analysis but whose heart weights were increased 2- to 3-fold as compared with that of WT age-matched controls, that showed myocardial disarray, or that were transgenic-positive by PCR analysis.

The sensitivity, specificity, and predictive values of the method were calculated by using Prism (GraphPad). A Pearson product-moment correlation matrix was used to identify significant

relationships among the independent variables (ECG and echocardiographic parameters, heart weights).Combined WT and ErbB2$^{tg}$ data were used to evaluate the power of various ECG parameters to distinguish between WT and ErbB2$^{tg}$ mice, whereas data from individual WT and ErbB2$^{tg}$ mice were used to evaluate the ability of ECG parameters to predict heart weight in individual animals.

## Results

**ErbB2 overexpression caused significant cardiac hypertrophy.** When compared with their WT littermates (Figure 2 A, C, and E), ErbB2$^{tg}$ mice had enlarged LV, interventricular septa, right ventricles, and atria, typical of concentric hypertrophy (Figure 2 B, D, F). Early in our characterization of ErbB2$^{tg}$ mice, we found that heart weight correlated 100% with genotype. For example, in 7- to 8-wk-old female mice, heart weight in WT mice ranged from 85 to 133 mg, whereas in transgenic mice, heart weight ranged from 203 to 408 mg. Male hearts are slightly larger in both WT (92 to 155 mg) and ErbB2$^{tg}$ (233 to 462 mg) mice.

**ECG features of cardiac hypertrophy in ErbB2$^{tg}$mice.** To determine whether the anatomic changes in the hypertrophied hearts of ErbB2$^{tg}$ mice induced distinctive electrocardiographic features, we compared ECG analyses between WT and transgenic littermates. Representative ECG tracings are presented (Figure 3), and averaged ECG parameters are listed in Table 1. Compared with those of WT mice (Figures 3 A and 4), the ECG of ErbB2$^{tg}$ mice (Figures 3 B and C, and 4) is characterized by higher P- and R-wave amplitudes, wider QRS complex, and repolarization changes (prolonged $QT_c$ interval and electrophysiologic LV strain pattern, consisting of T-wave inversion and ST depression). In addition, most ErbB2$^{tg}$ mice showed $QT_c$ prolongation (Figure 4 G). Therefore, the ErbB2$^{tg}$ mouse model of cardiac hypertrophy is associated with an ECG pattern characterized by increased voltage, widened QRS complex, prolonged $QT_c$ interval, and LV strain.

In addition to these common ECG changes, other distinctive changes were present in some ErbB2$^{tg}$mice but not in any of their WT littermates. These changes include shortened PR interval (less than 20 ms, approximately 60% of ErbB2$^{tg}$ mice), ECG features suggestive of left axis deviation ($R_{II} < R_I$, 7.7% of ErbB2$^{tg}$ mice; Figure 3 C, Table 2), and variable QRS morphologies (11.4% of ErbB2$^{tg}$ mice; Figure 5 C, Table 2).

**ECG parameters enabled the classification of ErbB2$^{tg}$ compared with WT mice.** To determine whether ECG parameters predicted anatomic heart parameters, thus allowing us to assign genotype according to a characteristic ECG phenotype, we performed Pearson's correlation matrix analyses of ECG data compared with heart weight as normalized to body weight. When combined WT and ErbB2$^{tg}$ data were used to evaluate the power of various ECG parameters to distinguish between WT and ErbB2$^{tg}$mice, the following parameters (in order of significance) correlated with normalized heart weight:$QT_c$ interval (r = 0.86), QRS interval (r = 0.81), ST height (r = –0.78), R amplitude (r = 0.77), P amplitude (r = 0.7), and PR interval (r = –0.53; Table 3, Figure 6), whereas heart rate (r = 0.03) and P duration (r = 0.34) did not correlate with normalized heart weight (Table 3). In contrast, within the WT group, only R amplitude correlated (r = 0.65) with normalized heart weight (Table 3), and no correlation between any ECG parameter and normalized heart weight occurred within the ErbB2$^{tg}$ group (Table 3). Therefore, ECG analysis enables discrimination between the WT and ErbB2$^{tg}$ genotypes but does not predict heart weight in individual mice.

**ECG parameters correlated with echocardiographic measurements.** Next, we examined whether specific ECG parameters and specific echocardiographic measurements in WT andErbB2$^{tg}$ mice were predictive of each another. Overall, when all data from both genotypes were combined, the strongest correlation was between the echocardiographically determined thickness of the LV posterior wall and the following ECG parameters (in order of significance): ST height (r = –0.86), R amplitude (r = 0.81), and QRS interval (r = 0.75; Table 4).

Correlation of echocardiography-based estimation of LV mass with ECG parameters is of particular interest for evaluation of LV hypertrophy. When the combined data from both genotypes were evaluated, LV mass correlated with ST height (r = –0.80), R amplitude (r = 0.78), QRS interval (r = 0.68), PR interval (r = –0.58), P amplitude (r = 0.60), and P duration (r = 0.44; Table 4, Figure 7).

In the WT group, P duration correlated with the thickness of the LV anterior (r = –0.51) and posterior (r = –0.54) walls and with LV mass (r = –0.50), and QRS interval correlated with LV mass (r = 0.52; Table 4). In ErbB2$^{tg}$ mice, ST height correlated with LV anterior wall thickness (r = –0.66), and heart rate correlated with LV posterior wall thickness (r = –0.65; Table 4). Therefore, ECG and echocardiographic parameters strongly correlate in the combined group of WT and ErbB2$^{tg}$mice, whereas Pearson r coefficients (0.5 to 0.6) were not as predictive within either the WT- or ErbB2$^{tg}$-only groups.

**Age-related changes of ECG in mice with cardiac hypertrophy.** To evaluate whether ECG parameters vary as mice grow older, we performed ECG in ErbB2$^{tg}$ and WT mice at 1 to 2 mo of age (young) and then at 7 to 9 mo of age (old; Figure 8). Heart rates did not differ significantly between young and old mice (WT: young mice, 496 ± 159 bpm; old mice, 515 ± 126 bpm; ErbB2$^{tg}$: young, 591 ± 77 bpm; old, 512 ± 141 bpm).The following ECG parameters showed the strongest correlation with heart weight in young mice and were analyzed: $QT_c$ interval, QRS duration, ST height, R amplitude, P amplitude and PR interval. In WT mice, only R wave amplitude decreased significantly with age (young, 1.04 ± 0.2 mV; old, 0.80 ± 1.89 mV; $P = 0.0005$), whereas in ErbB2$^{tg}$ mice, the following parameters showed significant changes: $QT_c$ interval (young, 61.97 ± 5.49 ms; old, 53.14 ± 10.37 ms; $P = 0.0023$); ST height (young, –0.4 ± 0.3 mV; old, –0.04 ± 0.19 mV; $P < 0.0001$); R amplitude (young, 2.83 ± 1.7 mV; old, 1.34 ± 0.66 mV; $P = 0.0065$); P amplitude (young, 0.41 ± 0.27 mV; old, 0.20 ± 0.09 mV; $P = 0.0293$); and PR interval (young, 21.18 ± 7.18; old, 31.06 ± 12.36 ms; $P = 0.0224$).

**Development of criteria for evaluation of cardiac hypertrophy in mice.** Based on regression data analysis, we determined the criteria that allowed us to phenotypically distinguish between WT and ErbB2$^{tg}$ mice (Table 5). Similarly to those in human HCM cases, we determined that ErbB2$^{tg}$ mice most frequently had repolarization changes, and other characteristic findings included increased P and R waves amplitudes, shortened PR and prolonged $QT_c$ intervals. The most sensitive parameter was $QT_c$ length, and the most specific parameters were P- and R- wave amplitude, QRS duration, and ST height. Using these criteria, we were able to correctly determine the genotype of 98.8% of mice, whereas the genotype of the remaining 1.2% (33 of 2671) of mice was unclear according to the ECG, mainly due to electrical noise during recording because additional tracings

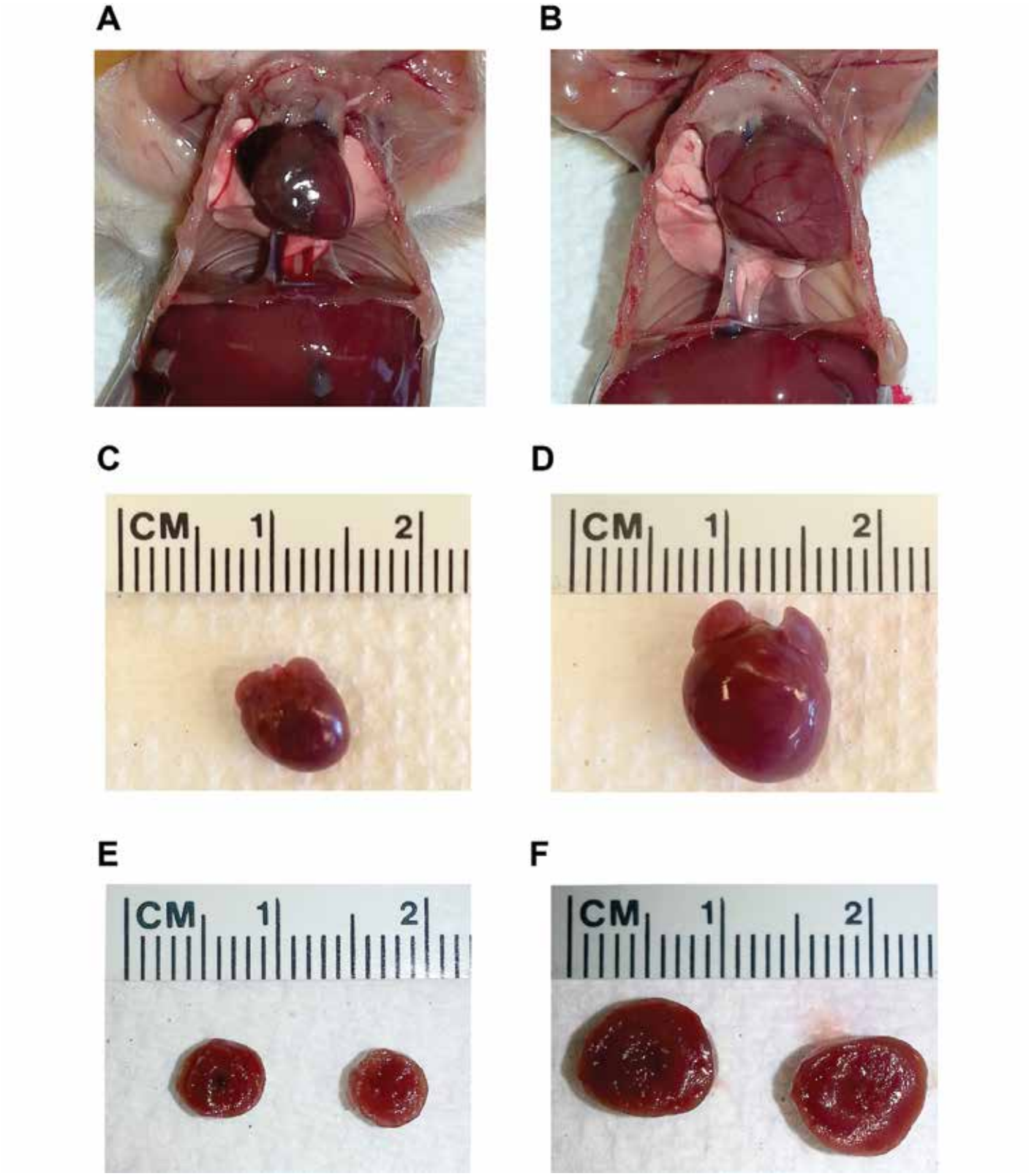


**Figure 2.** Cardiac hypertrophy in ErbB2$^{tg}$ mice. The hearts of (A) WT and (B) ErbB2$^{tg}$ mice in situ. Gross morphology of hearts in (C) WT and (D) ErbB2$^{tg}$ mice. Transverse sections of the hearts in (E) WT and (F) ErbB2$^{tg}$ mice.

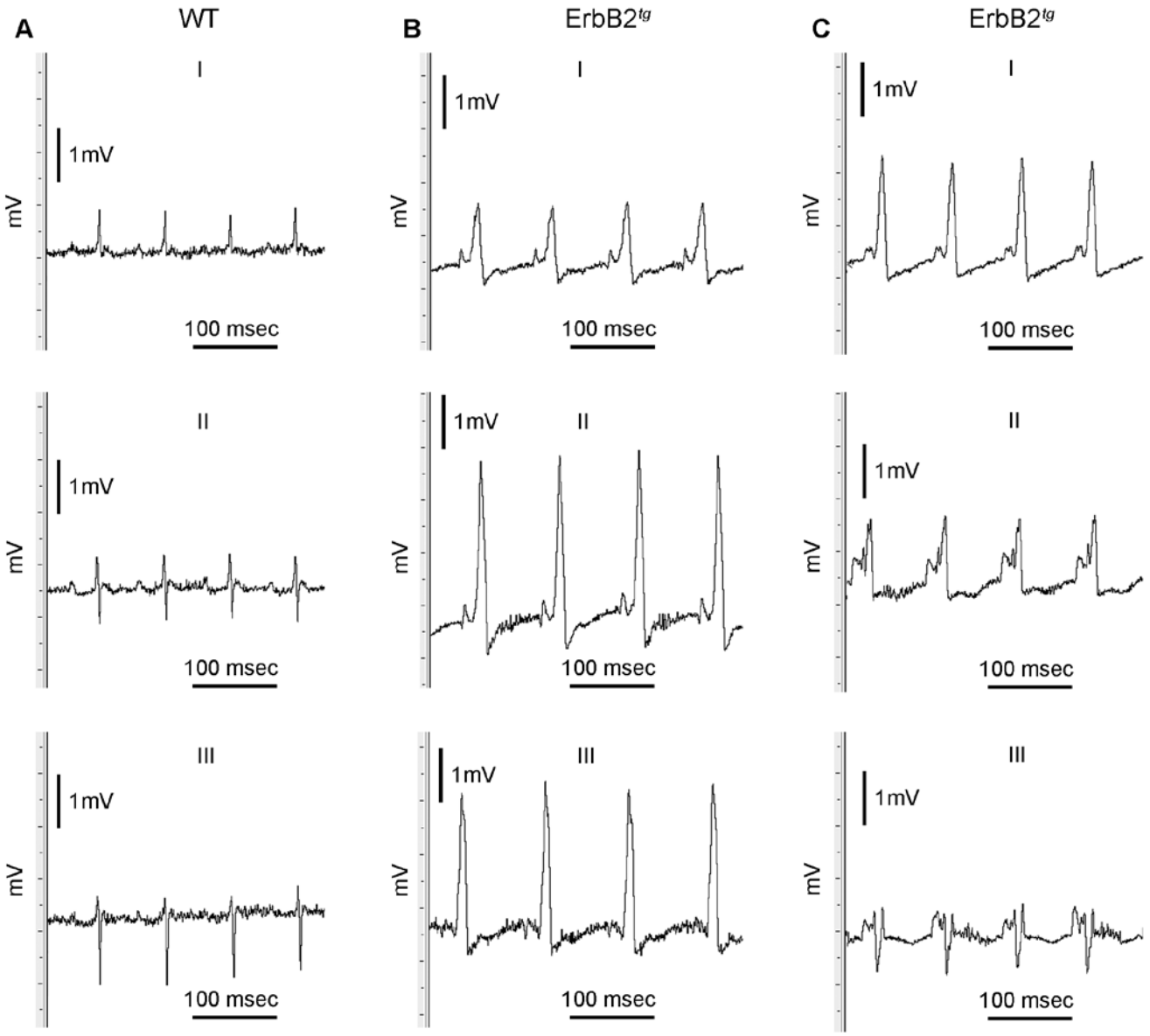


**Figure 3.** ECG tracings in WT and ErbB2$^{tg}$ mice. Representative 3-lead ECG tracings in (A) WT, (B) ErbB2$^{tg}$ (intermediate electrical axis of the heart), and (C) ErbB2$^{tg}$ (left axis deviation) mice.

were diagnostic. In addition, the initial ECG in some of the 33 mice were positive in terms of criteria for minor characteristics but not major ECG criteria. In these cases, the suspected genotype was recorded, but the possibility of its being incorrect was noted; these mice generally were excluded from subsequent experiments. In addition, we also determined the false-positive and false-negative rates in a subset ($n$ = 352) of mice of known ErbB2$^{tg}$ genotype (heart weight, distinctive myocardial disarray, and PCR results). The false-positive rate was 2.08%, due to 3 WT mice that were thought to be ErbB2 mice due to difficulty in reading the ear markings of one litter. The false-negative rate was 0.48%, due to 1 ErbB2$^{tg}$ mouse among 208 WT mice that tested negative for ErbB2$^{tg}$ genotype according to ECG criteria but that was transgenic according to heart weight and pathology. Again, this situation resulted from earmarkings that were difficult to distinguish.

**Table 1.** Values (mean ± 1 SD) ECG parameters in WT and ErbB2$^{tg}$ mice

| | WT | ErbB2$^{tg}$ |
|---|---|---|
| Heart rate (bpm) | 608 ± 112 | 596 ± 88 |
| RR interval (ms) | 102 ± 20 | 105 ± 18 |
| PR interval (ms) | 27.62 ± 3.51 | 20.17 ± 8.27[b] |
| P duration (ms) | 8.81 ± 4.36 | 12.74 ± 4.61[a] |
| QRS interval (ms) | 7.18 ± 0.83 | 13.12 ± 2.53[c] |
| $QT_c$ interval (ms) | 30.1 ± 11.91 | 61.57 ± 4.95[c] |
| P amplitude (mV) | 0.12 ± 0.04 | 0.41 ± 0.17[c] |
| R amplitude (mV) | 1.09 ± 0.36 | 2.96 ± 0.88[c] |
| ST height (mV) | 0.13 ± 0.04 | –0.42 ± 0.26[c] |

Values differed significantly ([a]$P < 0.05$; [b]$P < 0.01$; [c]$P < 0.0001$) between groups.

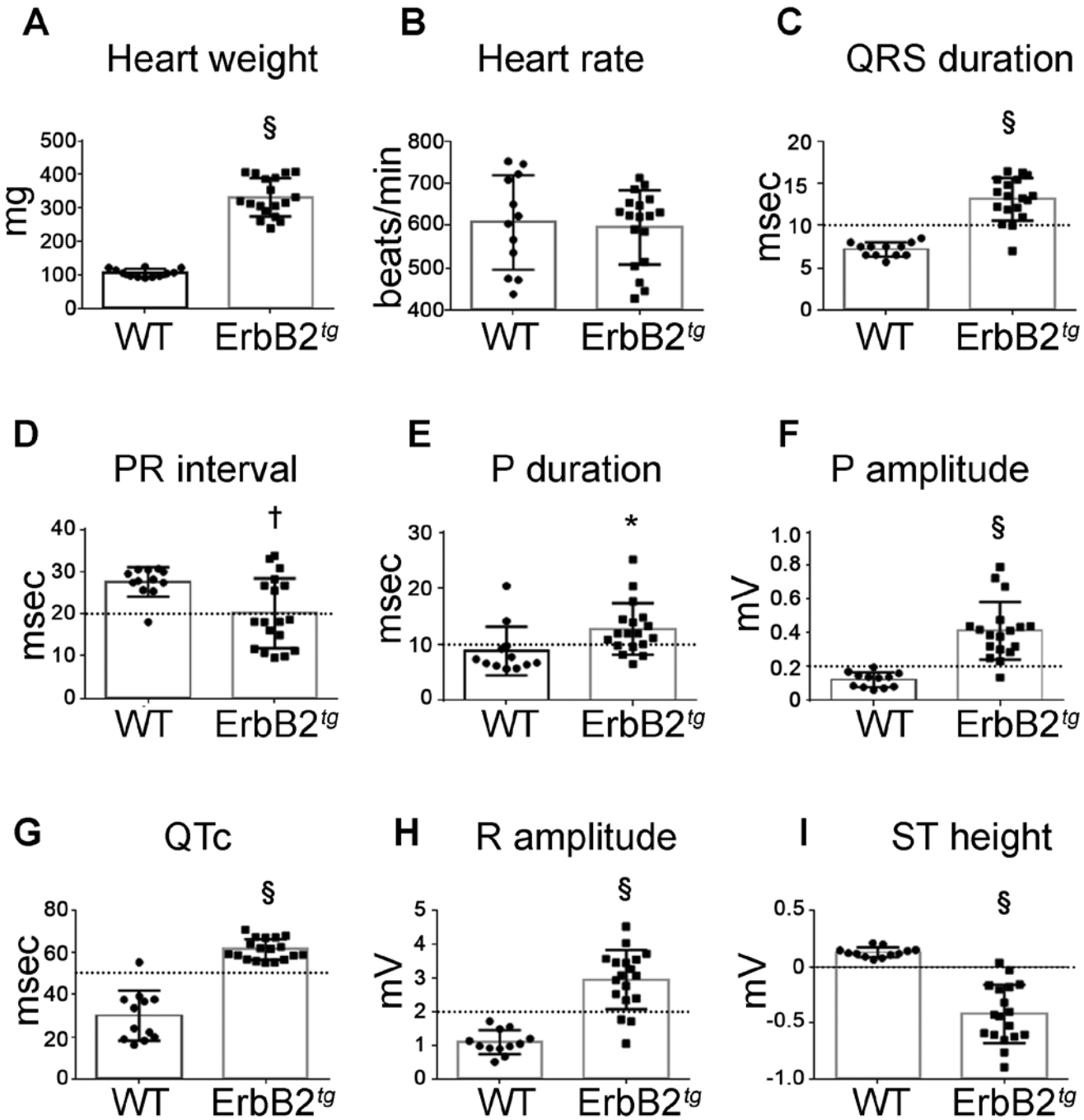


**Figure 4.** ECG comparison of WT and ErbB2$^{tg}$ mice. (A) Heart weights and (B through I) ECG parameters in the WT and ErbB2$^{tg}$ mice.*, $P < 0.05$; †, $P < 0.01$; and §, $P < 0.0001$ (Student unpaired $t$ test).

**Table 2.** Incidence of left axis deviation and variable QRS morphologies[a]

| | Male mice | | Female mice | | Total mice | |
|---|---|---|---|---|---|---|
| | *n* | % | *n* | % | *n* | % |
| Total mice | 468 | 47.1 | 525 | 52.9 | 993 | 100 |
| WT mice | 336 | 33.8 | 359 | 36.2 | 695 | 70 |
| ErbB2$^{tg}$ mice | 132 | 13.3 | 166 | 16.7 | 298 | 30 |
| ErbB2$^{tg}$ mice with left axis deviation | 9 | 6.8 | 14 | 8.4 | 23 | 7.7 |
| ErbB2$^{tg}$ mice with variable QRS morphologies | 15 | 11.4 | 19 | 11.4 | 34 | 11.4 |

[a]These features were present only in ErbB2$^{tg}$ mice.

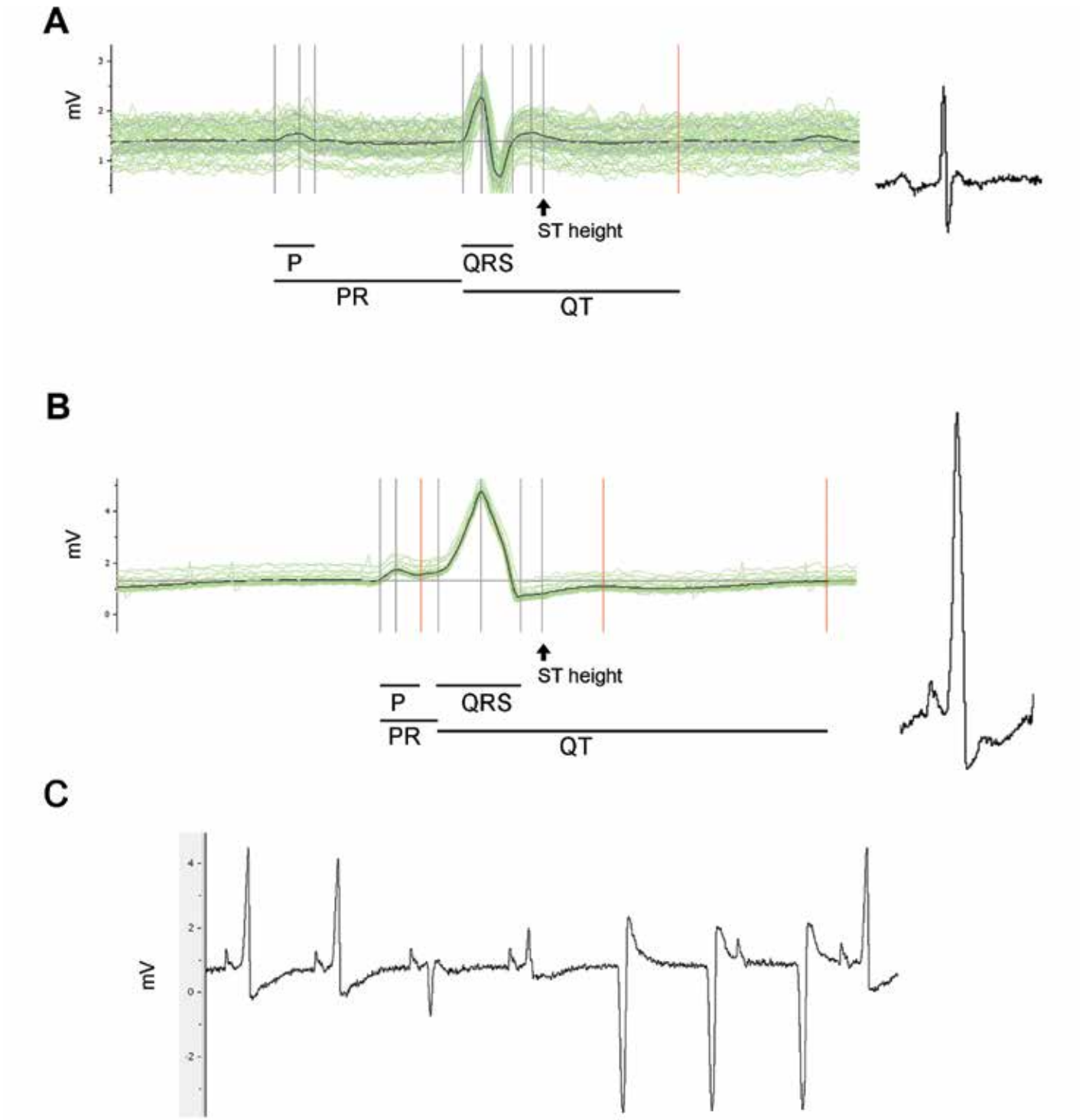


**Figure 5.** ECG evaluation in WT and ErbB2$^{tg}$ mice. Determination and averaging of individual ECG parameters in (A) WT and (B) ErbB2$^{tg}$ mice. (C) Variable QRS morphologies in ErbB2$^{tg}$ mice.

## Discussion

Previously we demonstrated that cardiac ErbB2 receptor tyrosine kinase overexpression results in the development of significant cardiac hypertrophy in mice,[47] similar in cardiac mass to overexpression of IGFβ1,[39] IGF-R1,[27] AKT,[26] and PI3K.[28,44] Using ErbB2$^{tg}$ mice and their WT littermates, we measured specific ECG parameters and related them to anatomic changes due to ErbB2-induced cardiac hypertrophy. On the basis of these findings, we established ECG phenotyping criteria for cardiac hypertrophy. We developed an inexpensive and time-efficient method to predict the genotype from the ECG phenotype; this method could be explored in other rodent models of cardiac hypertrophy.[26-28,39,44]

**Table 3.** Pearson product–moment correlation between heart weight (normalized to body weight) and ECG parameters in WT and ErbB2$^{tg}$ mice

| | Data used to determine power of ECG parameter to differentiate between genotypes | | |
|---|---|---|---|
| | WT and ErbB2$^{tg}$ data combined | WT data only | ErbB2$^{tg}$ data only |
| Heart rate (bpm) | −0.04 | −0.13 | 0.1 |
| PR interval (ms) | −0.5[b] | −0.24 | −0.15 |
| P duration (ms) | 0.34 | −0.16 | −0.16 |
| QRS interval (ms) | 0.77[c] | −0.42 | −0.03 |
| QT interval (ms) | 0.84[c] | −0.44 | 0.25 |
| P amplitude (mV) | 0.69[c] | 0.25 | −0.05 |
| R amplitude (mV) | 0.82[c] | 0.65[a] | 0.3 |
| ST height (mV) | −0.81[c] | −0.09 | −0.28 |

Values differed significantly ([a]$P < 0.05$; [b]$P < 0.01$; [c]$P < 0.0001$) between genotypes.

Using lead II ECG recording, the standard lead for most mouse ECG studies,[3,5,10,13] we were able to predict ErbB2 transgene expression in individual mice, which resulted in a distinct hypertrophic phenotype that was easily recognized on ECG tracings with minimal training. Our method yields a high-quality recording without anesthesia-related ECG changes (for example, bradycardia), with minimal handling of the mouse. Technically, ECG recording for genotyping purposes required less than 1 min per mouse (3 to 5 min per cage of 5 mice), including transporting the cage from the cage rack to the adjacent laminar flow hood, spraying the cage with disinfecting solution, handling the mice, using the ear puncher to label the mice, performing ECG, recording the result in the colony census spreadsheet and on the cage identification card, transporting the cage back to the cage rack, saving the LabChart file, and opening a new file for the next cage.

ErbB2 overexpression in the heart results in the development of significant cardiac hypertrophy that involves both ventricles and atria. We examined 2 age groups (1 to 3 mo and 7 to 9 mo) each of male and female WT and ErbB2$^{tg}$mice and discovered several ECG abnormalities in the ErbB2$^{tg}$ mice: high P and R amplitudes, wide QRS complexes, and repolarization changes including prolonged $QT_c$ intervals and electrophysiologic LV strain pattern (inverted T waves and ST depression).Repolarization changes in ErbB2$^{tg}$ mice may be due to primary alteration in repolarization in hypertrophied muscle or to relative subendocardial ischemia.[19,20,43] On a cellular level, changes in action potential duration in cardiomyocytes have been suggested as basis for the T-wave inversion in the rat model of isoproterenol-induced cardiac hypertrophy.[45] In our study, repolarization changes appeared to have the highest correlation with cardiac mass determined by other methods: ST-segment and T wave abnormalities showed the greatest correlation with the echocardiographically determined LV mass, whereas the $QT_c$ interval correlated most with heart weight.

The ECG changes in ErbB2$^{tg}$ mice are characteristic of LV hypertrophy in humans with HCM (short PR interval, extremely large QRS voltage, T-wave inversion).[12] Generally, T-wave inversion and ST-interval depression are suggestive of acute myocardial infarction.[9] In cases of confirmed LV hypertrophy, in addition to voltage criteria characteristic of LV hypertrophy, T-wave and ST-interval changes are attributed to hypertrophy. Similar variable QRS morphologies, suggestive of multiple accessory atrioventricular connections, occurred in a mouse model of cardiac hypertrophy that was due to mutated *PRKAG2*$^{N488I}$ overexpression.[4] Interestingly, in clinical practice, a shortened PR (PQ) interval (with or without a δ-wave) is most often observed in patients with lysosomal storage diseases who have cardiac hypertrophy.[22,38]

We compared ECG with echocardiography parameters because echocardiography is more widely used in both human and mouse cardiology. In human clinical practice, echocardiography is considered to be a gold standard for the diagnosis of hypertrophic cardiomyopathy, although other more precise but more costly methods are available, including cardiac MRI.[37,49] In human patients undergoing ECG, ST-segment abnormalities and inverted T waves occur in most patients with a diagnosis of hypertrophic cardiomyopathy,[12,25] and the LV strain pattern has been shown to correlate with echocardiographic LV mass and corrected $QT_c$ duration.[33,34,41] Evaluation of the QT interval together with more common voltage criteria adds to the specificity of ECG diagnosis of LV hypertrophy.[42] Although in human patients, the sensitivity of the strain pattern as a measure of LV hypertrophy is low (3.85% to 50%), specificity ranges from 89.8% to 100%,[32] and strain pattern, but not Sokolow–Lyon voltage criteria (more commonly used), was shown to be associated with the presence and predictive of anatomic LV hypertrophy.[11]

In mice, we compared ECG findings between young (1 to 2 mo) and older (7 to 9 mo) mice and observed decreases in P- and R-wave amplitudes that correlated with age-related heart mass loss in ErbB2$^{tg}$ mice. Decreased ECG voltages might be attributed to age-associated progressive cardiac fibrosis in ErbB2$^{tg}$ mice. Interestingly, PR-interval duration was increased in old compared with young mice. Although we did not identify the etiology of the shortened PR interval in some ErbB2$^{tg}$ mice, possible causes include accessory atrioventricular connections; the developing fibrosis may affect these accessory pathways, contributing to delayed atrioventricular conduction in older mice.

Cardiac hypertrophy in ErbB2$^{tg}$ mice is characterized by cardiomyocyte hypertrophy, myofiber disarray, and interstitial fibrosis that increases with age.[47] Hypertrophy in ErbB2$^{tg}$ mice hearts does not progress to overt dilation and heart failure, consistent with the clinical scenario in humans with HCM. Mutations of the *ErbB2* gene have not yet been studied in humans with HCM. Many rodent HCM models lack the specific ECG features, hypertrophy, and pathology often observed in human HCM. Most cases of HCM in humans are linked to more than 1500 mutations in 11 sarcomeric proteins, with multiple mutations in some patients.[24] Another cause for HCM in human patients, when sarcomeric gene mutations are not present, is lysosomal storage diseases,[22,31] and some examples can mimic HCM associated with sarcomeric gene mutation.[8] Human patients with HCM due to sarcomeric genes mutations or lysosomal storage diseases share electrocardiographic features with ErbB2$^{tg}$ mice, including increased P- and R-waves voltages and durations (due to increased myocardial mass) and repolarization changes (ECG strain pattern, $QT_c$ prolongation). To date, few of the mouse HCM models share this distinctive group of features.

Using ECG analysis to determine phenotype bears various limitations. The method is applicable after gross anatomic changes occur, which become a substrate for the ECG-associated changes, and is sufficient to distinguish between WT and ErbB2$^{tg}$ mice. This increase in cardiac mass becomes significant after day 11 to 12 of life; because the increased rate of false negatives in younger mice, we wait to perform ECG when mice

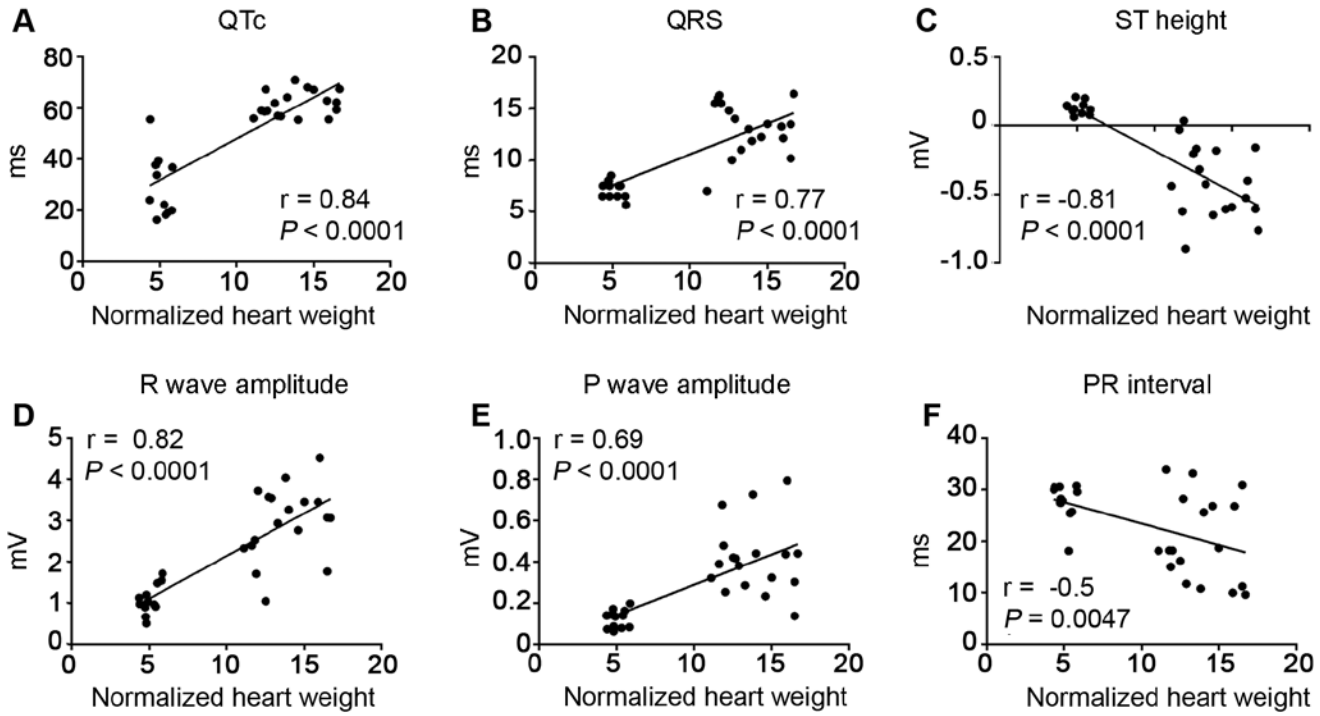


**Figure 6.** Correlation analysis of the normalized heart weight and ECG parameters in WT and ErbB2$^{tg}$ mice. (A) QT interval. (B) QRS width. (C) ST height. (D) R-wave amplitude. (E) P-wave amplitude. (F) PR interval.

**Table 4.** Pearson product–moment correlation matrix of echocardiographic and electrocardiographic parameters in WT and ErbB2$^{tg}$ mice

| | LWAW | | | LVPW | | | LV mass | | |
|---|---|---|---|---|---|---|---|---|---|
| | WT and ErbB2$^{tg}$ data combined | WT data only | ErbB2$^{tg}$ data only | WT and ErbB2$^{tg}$ data combined | WT data only | ErbB2$^{tg}$ data only | WT and ErbB2$^{tg}$ data combined | WT data only | ErbB2$^{tg}$ data only |
| Heart rate (bpm) | −0.17 | 0.12 | −0.23 | −0.27 | 0.18 | −0.65$^{b}$ | −0.15 | 0.33 | −0.25 |
| PR interval (ms) | −0.67$^{d}$ | −0.28 | −0.23 | −0.63$^{d}$ | −0.44 | −0.02 | −0.58$^{c}$ | −0.25 | 0.08 |
| P duration (ms) | 0.4$^{a}$ | −0.51$^{a}$ | −0.39 | 0.46$^{b}$ | −0.54$^{a}$ | −0.48 | 0.44$^{a}$ | −0.5$^{a}$ | −0.32 |
| QRS interval (ms) | 0.75$^{d}$ | 0.36 | 0.27 | 0.69$^{d}$ | 0.45 | −0.09 | 0.68$^{d}$ | 0.52$^{a}$ | −0.04 |
| QT interval (ms) | 0.44$^{a}$ | −0.06 | −0.09 | 0.4$^{a}$ | 0.08 | −0.33 | 0.34 | −0.33 | −0.36 |
| P amplitude (mV) | 0.64$^{d}$ | 0.09 | −0.15 | 0.63$^{d}$ | 0.08 | −0.39 | 0.6$^{c}$ | 0.34 | −0.39 |
| R amplitude (mV) | 0.81$^{d}$ | −0.21 | 0.38 | 0.72$^{d}$ | −0.4 | −0.18 | 0.78$^{d}$ | −0.01 | 0.21 |
| ST height (mV) | −0.86$^{d}$ | 0.26 | −0.66$^{b}$ | −0.81$^{d}$ | −0.08 | −0.27 | −0.8$^{d}$ | −0.19 | −0.33 |

LVAW, left venticular anterior wall; LVPW, left ventricular posterior wall, LVmass, left ventricular mass.
Values differed significantly ($^{a}P < 0.05$; $^{b}P < 0.01$; $^{c}P < 0.001$; $^{d}P < 0.001$) between genotypes.
*$P < 0.05$, **$P < 0.01$, ***$P < 0.001$, ****$P < 0.0001$.

are weaned at 3 to 4 wk of age. Heart weight begins to differ between WT and ErbB2$^{tg}$ mice on day 7 to 9 of life. Therefore, our ECG method is not applicable for determining the genotype in 1- to 3-day-old mice. Instead, to isolate cardiomyocytes from the 2 genotypes, we sample the tail tips of newborn mice, isolate DNA, and use PCR to determine the genotype of the pups. In addition, in studies in which drugs can be used to prevent or reduce hypertrophy, analysis of DNA for genotyping is done at 1 to 3 days after birth. Therefore, phenotyping by using the ECG method is not always superior to the DNA-based method.

Our brief literature review suggests that our model offers both advantages and disadvantages in regard to its HCM-specific ECG features, which are not always seen in other models of HCM. Therefore, although we present this model of concentric cardiac hypertrophy as one of a few animal models that mimics HCM that is accompanied by ECG changes, the ECG characteristics we present here may not be specific for other rodent models of HCM, particularly those modeling asymmetric, apical, right ventricular, restrictive, or other types of hypertrophy.

Although our method is cost-efficient over the long term (years) in colony management and for large colonies, it may not be as useful for small projects that require dozens (but not hundreds to thousands) of mice or for labs that do not anticipate using the data acquisition system for other projects. In addition, the described method does not distinguish between homozygotic

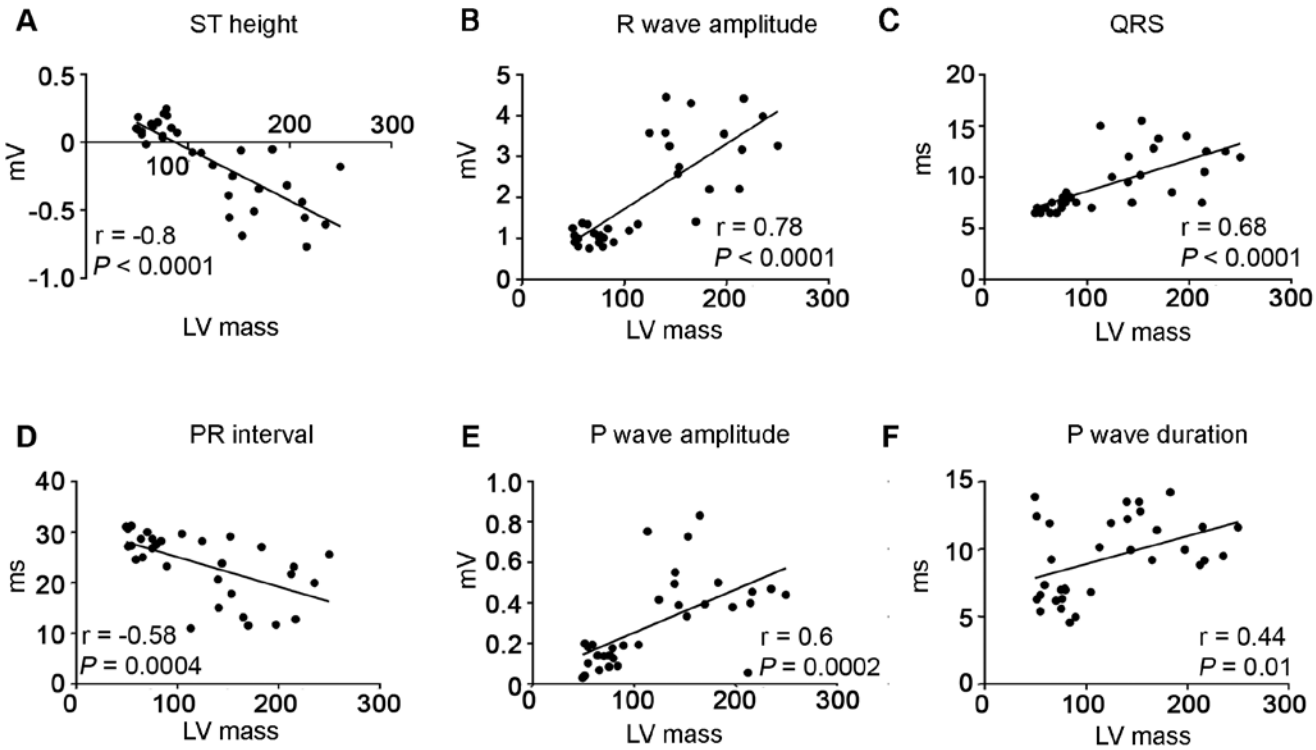


**Figure 7.** Correlation analysis of echocardiographic LV mass and ECG parameters in WT and ErbB2$^{tg}$ mice. (A) ST height. (B) R-wave amplitude. (C) QRS width. (D) PR interval. (E) P-wave amplitude. (F) P-wave duration.

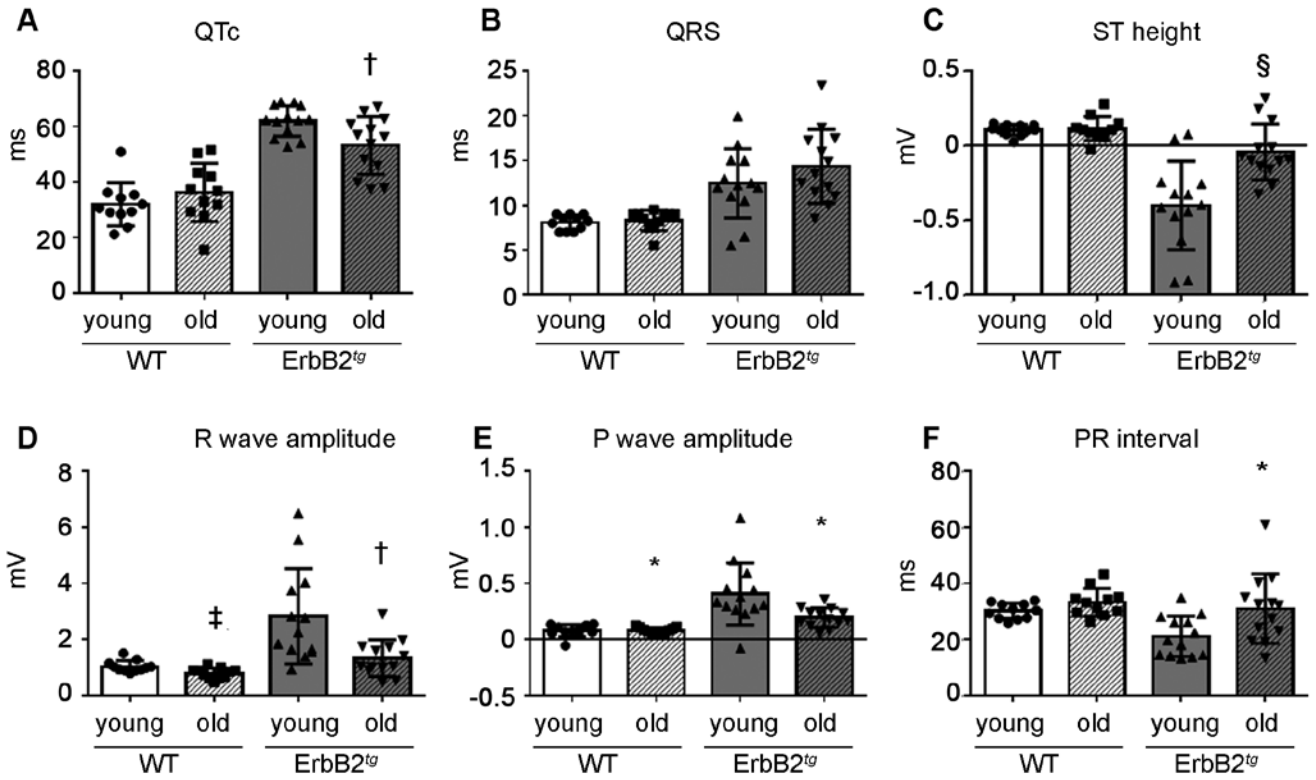


**Figure 8.** Longitudinal comparison of ECG parameters in mice of different ages. ECG parameters recorded in 1- to 2-mo-old (young) and 7- to 9-mo-old (old) WT and ErbB2$^{tg}$ mice. (A) QTc. (B) QRS width. (C) ST height. (D) R-wave amplitude. (E) P-wave amplitude. (F) PR interval. *, $P < 0.05$; †, $P < 0.01$; ‡, $P < 0.001$, §, $P < 0.0001$ (paired Student $t$ test).

**Table 5.** Criteria for determination of cardiac hypertrophy in ErbB2$^{tg}$ mice

| | Value | Sensitivity (%) | Specificity (%) | Positive predictive value | Negative predictive value |
|---|---|---|---|---|---|
| PR interval | ≤20 ms | 61.1 | 91.7 | 91.7 | 61.1 |
| P wave amplitude | >0.2 mV | 94.4 | 100 | 100 | 92.3 |
| P wave duration | >10 ms | 72.2 | 83.3 | 86.6 | 66.6 |
| QRS duration | >10 ms | 94.4 | 100 | 100 | 92.3 |
| R wave amplitude | >2 mV | 83.3 | 100 | 100 | 80 |
| QT interval | >50 ms | 100 | 91.7 | 94.8 | 100 |
| ST height | <0 mV | 94.4 | 100 | 100 | 92.3 |

and heterozygotic transgenic mice, nor can it determine the transgene copy number.

In summary, we have developed a murine model of cardiac hypertrophy characterized by ECG features similar to those in human patients with HCM. These ECG features enabled us to separate WT mice from ErbB2$^{tg}$ littermates after weaning and reduced the costs and time needed relative to those required for standard genotyping methods.

## References

1. **Abraham TP, Jones M, Kazmierczak K, Liang HY, Pinheiro AC, Wagg CS, Lopaschuk GD, Szczesna-Cordary D.** 2009. Diastolic dysfunction in familial hypertrophic cardiomyopathy transgenic model mice. Cardiovasc Res **82:**84–92.
2. **Ahmad F, Arad M, Musi N, He H, Wolf C, Branco D, Perez-Atayde AR, Stapleton D, Bali D, Xing Y, Tian R, Goodyear LJ, Berul CI, Ingwall JS, Seidman CE, Seidman JG.** 2005. Increased α2 subunit-associated AMPK activity and PRKAG2 cardiomyopathy. Circulation **112:**3140–3148.
3. **Appleton GO, Li Y, Taffet GE, Hartley CJ, Michael LH, Entman ML, Roberts R, Khoury DS.** 2004. Determinants of cardiac electrophysiological properties in mice. J Interv Card Electrophysiol **11:**5–14.
4. **Arad M, Moskowitz IP, Patel VV, Ahmad F, Perez-Atayde AR, Sawyer DB, Walter M, Li GH, Burgon PG, Maguire CT, Stapleton D, Schmitt JP, Guo XX, Pizard A, Kupershmidt S, Roden DM, Berul CI, Seidman CE, Seidman JG.** 2003. Transgenic mice overexpressing mutant PRKAG2 define the cause of Wolff–Parkinson–White syndrome in glycogen storage cardiomyopathy. Circulation **107:**2850–2856.
5. **Becker DE.** 2006. Fundamentals of electrocardiography interpretation. Anesth Prog **53:**53–64.
6. **Bijvoet AG, van de Kamp EH, Kroos MA, Ding JH, Yang BZ, Visser P, Bakker CE, Verbeet MP, Oostra BA, Reuser AJ, van der Ploeg AT.** 1998. Generalized glycogen storage and cardiomegaly in a knockout mouse model of Pompe disease. Hum Mol Genet **7:**53–62.
7. **Bostick B, Yue Y, Duan D.** 2011. Phenotyping cardiac gene therapy in mice. Methods Mol Biol **709:**91–104.
8. **Brito D**, **Miltenberger-Miltenyi G**, **Moldovan O**, **Navarro C**, **Madeira HC**. 2014. Cardiac Anderson–Fabry disease: lessons from a 25-year follow-up. Rev Port Cardiol **33**:247.e1–247.e7.
9. **Carey MG, Ponivas SJ, Pelter MM.** 2006. Differentiating ST-segment strain pattern from acute ischemia. Am J Crit Care **15:**321–322.
10. **Du XJ, Gao XM, Wang B, Jennings GL, Woodcock EA, Dart AM.** 2000. Age-dependent cardiomyopathy and heart failure phenotype in mice overexpressing β2-adrenergic receptors in the heart. Cardiovasc Res **48:**448–454.
11. **Ehara S, Hasegawa T, Matsumoto K, Otsuka K, Yamazaki T, Iguchi T, Izumi Y, Shimada K, Yoshiyama M.** 2013. The strain pattern, and not Sokolow–Lyon electrocardiographic voltage criteria, is independently associated with anatomic left ventricular hypertrophy. Heart Vessels **29:**638–644.
12. **Elliott PM, Anastasakis A, Borger MA, Borggrefe M, Cecchi F, Charron P, Hagege AA, Lafont A, Limongelli G, Mahrholdt H, McKenna WJ, Mogensen J, Nihoyannopoulos P, Nistri S, Pieper PG, Pieske B, Rapezzi C, Rutten FH, Tillmanns C, Watkins H.** 2014. 2014 ESC guidelines on diagnosis and management of hypertrophic cardiomyopathy: the Task Force for the Diagnosis and Management of Hypertrophic Cardiomyopathy of the European Society of Cardiology (ESC). Eur Heart J **35:**2733–2779.
13. **Farraj AK**, **Hazari MS**, **Cascio WE**. 2011. The utility of the small rodent electrocardiogram in toxicology. Toxicol Soc **121**:11–30.
14. **Fox JG, Barthold S**, **Davisson M, Newcomer CE, Quimby FW, Smith A.** 2006. The mouse in biomedical research, 2nd ed. Volume 3: normative biology, husbandry, and models. New York (NY): Academic Press.
15. **Goldbarg AN, Hellerstein HK, Bruell JH, Daroczy AF.** 1968. Electrocardiogram of the normal mouse, *Mus musculus*: general considerations and genetic aspects. Cardiovasc Res **2:**93–99.
16. **Ho D, Zhao X, Gao S, Hong C, Vatner DE, Vatner SF.** 2011. Heart rate and electrocardiography monitoring in mice. Curr Protoc Mouse Biol **1:**123–139.
17. **Institute for Laboratory Animal Research**. 2011. Guide for the care and use of laboratory animals, 8th ed. Washington (DC): National Academies Press.
18. **Jimenez J, Tardiff JC.** 2011. Abnormal heart rate regulation in murine hearts with familial hypertrophic cardiomyopathy-related cardiac troponin T mutations. Am J Physiol Heart Circ Physiol **300:**H627–H635.
19. **Kawasaki T, Azuma A, Kuribayashi T, Taniguchi T, Miyai N, Kamitani T, Kawasaki S, Matsubara H, Sugihara H.** 2006. Resting ST-segment depression predicts exercise-induced subendocardial ischemia in patients with hypertrophic cardiomyopathy. Int J Cardiol **107:**267–274.
20. **Kawasaki T, Sugihara H.** 2014. Subendocardial ischemia in hypertrophic cardiomyopathy. J Cardiol **63:**89–94.
21. **Knollmann BC, Blatt SA, Horton K, de Freitas F, Miller T, Bell M, Housmans PR, Weissman NJ, Morad M, Potter JD.** 2000. Inotropic stimulation induces cardiac dysfunction in transgenic mice expressing a troponin T (I79N) mutation linked to familial hypertrophic cardiomyopathy. J Biol Chem **276:**10039–10048.
22. **Linhart A, Elliott PM.** 2007. The heart in Anderson–Fabry disease and other lysosomal storage disorders. Heart **93:**528–535.
23. **Maron BJ, Epstein SE, Roberts WC.** 1986. Causes of sudden death in competitive athletes. J Am Coll Cardiol **7:**204–214.
24. **Maron BJ, Maron MS.** 2014. The 25-year genetic era in hypertrophic cardiomyopathy: revisited. Circ Cardiovasc Genet **7:**401–404.
25. **Maron BJ, Wolfson JK, Ciro E, Spirito P.** 1983. Relation of electrocardiographic abnormalities and patterns of left ventricular hypertrophy identified by 2-dimensional echocardiography in patients with hypertrophic cardiomyopathy. Am J Cardiol **51:**189–194.
26. **Matsui T, Li L, Wu JC, Cook SA, Nagoshi T, Picard MH, Liao R, Rosenzweig A.** 2002. Phenotypic spectrum caused by transgenic overexpression of activated Akt in the heart. J Biol Chem **277:**22896–22901.

27. **McMullen JR, Shioi T, Huang WY, Zhang L, Tarnavski O, Bisping E, Schinke M, Kong S, Sherwood MC, Brown J, Riggi L, Kang PM, Izumo S.** 2003. The insulin-like growth factor 1 receptor induces physiological heart growth via the phosphoinositide 3 kinase (p110α) pathway. J Biol Chem **279:**4782–4793.
28. **McMullen JR, Shioi T, Zhang L, Tarnavski O, Sherwood MC, Kang PM, Izumo S.** 2003. Phosphoinositide 3 kinase (p110α) plays a critical role for the induction of physiological, but not pathological, cardiac hypertrophy. Proc Natl Acad Sci USA **100:**12355–12360.
29. **Mitchell GF, Jeron A, Koren G.** 1998. Measurement of heart rate and QT interval in the conscious mouse. Am J Physiol **274:**H747–H751.
30. **Moak JP, Kaski JP.** 2012. Hypertrophic cardiomyopathy in children. Heart **98:**1044–1054.
31. **O'Mahony C, Elliott P.** 2010. Anderson–Fabry disease and the heart. Prog Cardiovasc Dis **52:**326–335.
32. **Ogah OS, Oladapo OO, Adebiyi AA, Adebayo AK, Aje A, Ojji DB, Salako BL, Falase AO.** 2008. Electrocardiographic left ventricular hypertrophy with strain pattern: prevalence, mechanisms, and prognostic implications. Cardiovasc J Afr **19:**39–45.
33. **Okin PM, Devereux RB, Fabsitz RR, Lee ET, Galloway JM, Howard BV, Strong Heart S.** 2002. Quantitative assessment of electrocardiographic strain predicts increased left ventricular mass: the Strong Heart study. J Am Coll Cardiol **40:**1395–1400.
34. **Okin PM, Devereux RB, Nieminen MS, Jern S, Oikarinen L, Viitasalo M, Toivonen L, Kjeldsen SE, Julius S, Dahlof B.** 2001. Relationship of the electrocardiographic strain pattern to left ventricular structure and function in hypertensive patients: the LIFE (Losartan Intervention For Endpoint) study. J Am Coll Cardiol **38:**514–520.
35. **Ostman-Smith I, Wettrell G, Keeton B, Riesenfeld T, Holmgren D, Ergander U.** 2005. Echocardiographic and electrocardiographic identification of those children with hypertrophic cardiomyopathy who should be considered at high-risk of dying suddenly. Cardiol Young **15:**632–642.
36. **Panza JA, Maron BJ.** 1989. Relation of electrocardiographic abnormalities to evolving left ventricular hypertrophy in hypertrophic cardiomyopathy during childhood. Am J Cardiol **63:**1258–1265.
37. **Pennell DJ, Sechtem UP, Higgins CB, Manning WJ, Pohost GM, Rademakers FE, van Rossum AC, Shaw LJ, Yucel EK, Society for Cardiovascular Magnetic R, Working Group on Cardiovascular Magnetic Resonance of the European Society of Cardiology.** 2004. Clinical indications for cardiovascular magnetic resonance (CMR): Consensus Panel report. Eur Heart J **25:**1940–1965.
38. **Pochis WT, Litzow JT, King BG, Kenny D.** 1994. Electrophysiologic findings in Fabry's disease with a short PR interval. Am J Cardiol **74:**203–204.
39. **Reiss K, Cheng W, Ferber A, Kajstura J, Li P, Li B, Olivetti G, Homcy CJ, Baserga R, Anversa P.** 1996. Overexpression of insulin-like growth factor 1 in the heart is coupled with myocyte proliferation in transgenic mice. Proc Natl Acad Sci USA **93:**8630–8635.
40. **Richards AG, Simonson E, Visscher MG.** 1953. Electrocardiogram and phonogram of adult and newborn mice in normal conditions and under the effect of cooling, hypoxia, and potassium. Am J Physiol **174:**293–298.
41. **Salles G, Cardoso C, Nogueira AR, Bloch K, Muxfeldt E.** 2006. Importance of the electrocardiographic strain pattern in patients with resistant hypertension. Hypertension **48:**437–442.
42. **Salles G, Leocadio S, Bloch K, Nogueira AR, Muxfeldt E.** 2005. Combined QT interval and voltage criteria improve left ventricular hypertrophy detection in resistant hypertension. Hypertension **46:**1207–1212.
43. **Schwartzkopff B, Mundhenke M, Strauer BE.** 1998. Alterations of the architecture of subendocardial arterioles in patients with hypertrophic cardiomyopathy and impaired coronary vasodilator reserve: a possible cause for myocardial ischemia. J Am Coll Cardiol **31:**1089–1096.
44. **Shioi T, Kang PM, Douglas PS, Hampe J, Yballe CM, Lawitts J, Cantley LC, Izumo S.** 2000. The conserved phosphoinositide-3-kinase pathway determines heart size in mice. EMBO J **19:**2537–2548.
45. **Shipsey SJ, Bryant SM, Hart G.** 1997. Effects of hypertrophy on regional action potential characteristics in the rat left ventricle: a cellular basis for T-wave inversion? Circulation **96:**2061–2068.
46. **Sidhu JS, Rajawat YS, Rami TG, Gollob MH, Wang Z, Yuan R, Marian AJ, DeMayo FJ, Weilbacher D, Taffet GE, Davies JK, Carling D, Khoury DS, Roberts R.** 2005. Transgenic mouse model of ventricular preexcitation and atrioventricular reentrant tachycardia induced by an AMP-activated protein kinase loss-of-function mutation responsible for Wolff–Parkinson–White syndrome. Circulation **111:**21–29.
47. **Sysa-Shah P, Xu Y, Guo X, Belmonte F, Kang B, Bedja D, Pin S, Tsuchiya N, Gabrielson K.** 2012. Cardiac-specific overexpression of epidermal growth factor receptor 2 (ErbB2) induces prosurvival pathways and hypertrophic cardiomyopathy in mice. PLoS ONE **7:**e42805.
48. **Tanaka N, Dalton N, Mao L, Rockman HA, Peterson KL, Gottshall KR, Hunter JJ, Chien KR, Ross J Jr.** 1996. Transthoracic echocardiography in models of cardiac disease in the mouse. Circulation **94:**1109–1117.
49. **To AC, Dhillon A, Desai MY.** 2011. Cardiac magnetic resonance in hypertrophic cardiomyopathy. JACC Cardiovasc Imaging **4:**1123–1137.
50. **Tsoutsman T, Kelly M, Ng DC, Tan JE, Tu E, Lam L, Bogoyevitch MA, Seidman CE, Seidman JG, Semsarian C.** 2008. Severe heart failure and early mortality in a double-mutation mouse model of familial hypertrophic cardiomyopathy. Circulation **117:**1820–1831.
51. **Wehrens XH, Kirchhoff S, Doevendans PA.** 2000. Mouse electrocardiography: an interval of 30 years. Cardiovasc Res **45:**231–237